

The super-resolution of linear structures in image data

Michael P. Egan

*National Geospatial-Intelligence Agency
Basic and Applied Research Office*

ABSTRACT

Super-resolution of images, particularly the separation of point sources within the Rayleigh limit of an optical system, has been empirically and theoretically proved. Issues remain, however, around the ability to perform true super-resolution of structure within extended objects. Puschmann and Kneer [1] conclude that “super-resolution cannot be achieved for extended objects which are not band limited.” They do find that sharpening by contrast enhancement was possible in extended images. Examination of the theoretical work of Donoho [2] suggests the possibility of resolving linear structures under certain conditions. The resolution enhancement is only possible in the direction normal to the feature’s length vector. I discuss here the required conditions for super-resolution of these objects and propose a modification of the Magain, Courbin and Sohy (MCS) method [3] that allows super-resolved reconstruction of linear features.

1. INTRODUCTION

In a previous paper (Egan [4]) examined the MCS method for super-resolution reconstruction of astronomical imaging as applied to data from the Midcourse Space Experiment (MSX). The MCS method seeks a higher resolution model of data by minimizing a function consisting of a data integrity term and a regularization term. In the MCS formulation this takes the form

$$S = \sum_{i=1}^N \frac{1}{\sigma_i^2} \left[\sum_{j=1}^N t_{ij} f_j - d_i \right]^2 + \lambda H(\mathbf{f})$$

where the first term is the data integrity term which is a χ^2 term quantifying the uncertainty weighted difference between the modeled true image, $\mathbf{t} \otimes \mathbf{f}$ and the measured data, \mathbf{d} . In this formulation, \mathbf{f} is the super-resolved image, which is convolved with a kernel \mathbf{t} that blurs the super-resolved image to the inferior resolution of the measured data.

The second term in the above equation – the regularization function - contains a Lagrange multiplier, λ , and a smoothing function, $H(f)$. The smoothing term can generally be thought of as a constraint on the reconstructed image, and the form it takes drives the nature of the solution. Unconstrained, the solution to the inverse problem has a variety of plausible solutions; the regularization function provides a criterion to determine a stable and unique solution. [2] Many regularization methods, such as Maximum Entropy, and maximum likelihood are global constraints. While these can solve some of the ringing artifacts, they are problematic in that they mathematically couple regions in the solution that are clearly not physically related. This manifests itself in photometric errors in the deconvolution solution and in serving to smooth sources that should be sharp.

More recent developments in deconvolution algorithms have found that local constraints on the smoothness of the background are more effective in reducing reconstruction artifacts than global constraints. Other work has shown that modeling point source components of an image separately from the extended background can result in superior performance of super-resolution imaging algorithms. These “two channel” methods model the form of the true light distribution as $f(\mathbf{x}) + h(\mathbf{x})$, where $f(\mathbf{x})$ is made up of the point sources in the observed field, and $h(\mathbf{x})$ is the extended component of the light distribution.

Magain, Courbin, and Sohy [1] have defined a two-channel deconvolution algorithm that avoids the ringing artifacts seen in some deconvolution algorithms. MCS shares characteristics with both the CLEAN algorithm and the two-

channel Richardson-Lucy algorithm [6], but differs from these in that the point source components are not modeled as delta functions. The MCS algorithm is based on the principle that sampled data cannot be fully deconvolved, i.e. yielding delta function-type point sources, without violating the sampling theorem.

In detail, the MCS technique seeks to minimize the function

$$S_2 = \sum \frac{1}{\sigma^2} \left[\mathbf{s} \otimes \left(\mathbf{h} + \sum_{k=1}^M a_k \mathbf{r}(\mathbf{x} - c_k) \right) - \mathbf{d} \right]^2 + \lambda \sum (\mathbf{h} - \mathbf{r} \otimes \mathbf{h})^2$$

where the point response function (PRF) of the original imaging system is represented by

$$\mathbf{p} = \mathbf{r} \otimes \mathbf{s}.$$

In the above equation the original data PRF, \mathbf{p} is assumed to be reproducible by the convolution of the PRF of the “ideal” system, \mathbf{r} , and the “deconvolution kernel” \mathbf{s} . The “ideal” system defines the resolution, and the image sampling needed for the super-resolution image. In practice, since \mathbf{p} is known, and \mathbf{r} is defined by the user, the deconvolution kernel, \mathbf{s} is solved for from these. Instead of a global technique, MCS opts for a regularization function that imposes local smoothness of the background component on the length scale of the PRF of the solution, \mathbf{r} .

This research on MCS has been motivated by the specific case of trying to enhance the resolution of low resolution infrared imagery from infrared surveys such as MSX and in the future, similar data that will be available from WISE. For these instruments, the need for a wide field of view drives the plate scale away from that required for true diffraction limited imaging. For example, the MSX instrument was a 33cm telescope, so at wavelengths of 10 μm the first zero of the Airy disk at $1.22\lambda/d$ would be at about 8 arcseconds. However, the plate scale of the MSX SPIRIT III instrument was 18 arcseconds per pixel; therefore the system resolution is driven by the pixel size and sampling rather than the diffraction limit of the optical system. I will refer to such optical systems in this paper as “low resolution systems”. Observatory instruments tend to match pixel size and the diffraction limit, for example the Spitzer Space Telescope IRAC instrument plate scale is 1.2 arcseconds per pixel, approximately equal to the diffraction limit at 4 μm and more than twice the diffraction limit at 10 μm for its 85cm aperture. Similarly, the Hubble WFPC2 camera has a plate scale of 0.04 arcseconds per pixel; about equal to the Airy disk first zero point in the visible spectrum.

2. PERFORMANCE OF MCS FOR POINT SOURCE SUPER-RESOLUTION

Before examining regularization schemes that improve the reconstruction of linear features, I would like to quantify the performance of the MCS method on the reconstruction of the point source map. It is expected that in the direction normal to linear features, the ability to resolve two parallel linear features should be similar to the ability of the MCS reconstruction to resolve point sources.

The ability of MCS to accurately reconstruct both the point source position and amplitude information for point sources will depend (in the noise-free case considered here) on the spatial distance between point sources. Since MCS seeks to reconstruct an image as seen by a superior (i.e. higher resolution) optical system than that of the original data, we expect the reconstruction to break down as the distance between point sources to be resolved approaches the Rayleigh limit for the new system.

A series of ten point source reconstructions were made of point source pairs starting at an image separation of ~ 3 times the Rayleigh limit of the “ideal” PRF \mathbf{r} and progressing closer to a final separation of ~ 0.1 times that limit. For the “original” low resolution image with PRF \mathbf{p} , the point sources were always unresolved, since the separation distance ranged from a maximum of 0.3 times the FWHM of \mathbf{p} to a minimum of < 0.01 FWHM of \mathbf{p} . Figure 1 shows the performance of the deconvolution in extracting the source intensities as a function of separation distance. The thin line is point source 1 and the thick line is point source 2. Figure 2 shows the deconvolved x (solid line) and y (dashed line) position difference from the true position (in pixels) for each source. For both position and amplitude, the performance is excellent for sources separated by at least the Rayleigh distance, A_0 , of the ideal system with PRF

r. When the sources are within the Rayleigh distance the method no longer is able to accurately determine the amplitude, or the position within the Rayleigh disk defined by **r**. This is the expected performance for point sources of this deconvolution method.

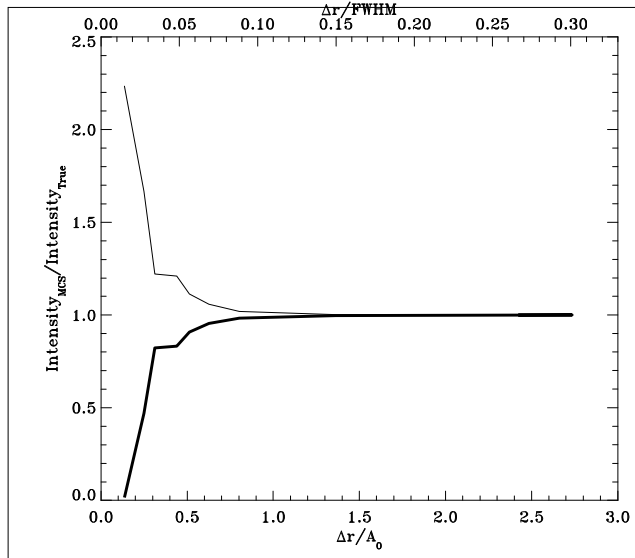


Figure 1 Point Source Amplitudes from Deconvolution

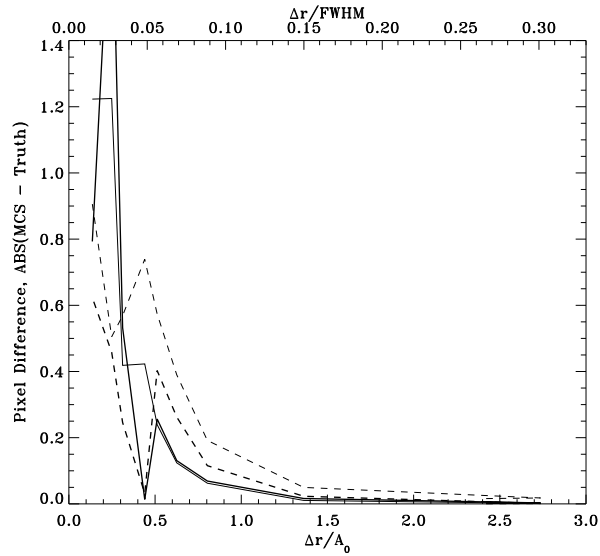


Figure 2 Point Source Position from Deconvolution

3. PERFORMANCE OF MCS ON EXTENDED SOURCES

This research has been motivated by the specific case of resolution enhancement of low resolution infrared imagery from infrared surveys such as MSX and in the future, similar data that will be available from WISE. For these instruments, the need for a wide field of view drives the plate scale away from that needed for diffraction limited performance. For example, the MSX instrument was a 33cm telescope, so at wavelengths of 10 μm the first zero of the Airy disk at $1.22\lambda/d$ would be at about 8 arcseconds. However, the plate scale of the MSX SPIRIT III instrument was 18 arcseconds per pixel; therefore the system resolution is driven by the pixel size and sampling rather than the diffraction limit of the optical system. Observatory instruments tend to match pixel size and the diffraction limit, for example the Spitzer Space Telescope IRAC instrument plate scale is 1.2 arcseconds per pixel, approximately equal to the diffraction limit at 4 μm wavelength and more than twice the diffraction limit at 10 μm

for its 85cm aperture. Similarly, the Hubble WFPC2 camera has a plate scale of 0.04 arcseconds per pixel, about equal to the Airy disk first zero point in the visible spectrum.

As the above section shows, point source super-resolution works very well even in cases where the imaging system does not achieve diffraction limited performance. However, the inherent resolution of the entire imaging system becomes very important in trying to recover the structure in the background. The lack of sampling at the true diffraction limit does reduce the ability of super-resolution algorithms to recover structure in the extended background, since all structures are blurred smooth to the sampling scale.

Because of this blurring, Egan's [3] reconstruction of a ring nebula around an MSX source was disappointing. While the general rhomboidal shape of the nebula, and the distinction between the low and high brightness regions of the nebula were recovered, the overall thinness, and the fine structure seen in the high resolution Spitzer image was not recovered by the MCS reconstruction. On reflection this is not surprising, since the extended emission left in the MSX map is smooth on scales consistent with the MSX PRF. The regularization term of the MCS method exists to smooth fluctuations smaller than the PRF of the reconstructed image. However, it does not contain any forcing term to drive any "peakiness" into the image other than already exists after the point sources are "removed".

Another way to think about this behavior is to recognize that MCS does not involve a true "deconvolution" step. This is by design in MCS, since it is recognized that deconvolution introduces ringing artifacts into the image. Such artifacts would then be amplified by the regularization term. Instead, MCS makes the initial assumption that the extended emission is the remaining image once the modeled point sources have been removed. Therefore the fluctuation scale is set by the subtraction of the point source model from the original image. If the extended emission is smooth on the scale of the original image PRF, p , as would be the case for linear features, the MCS regularization term enhances the peakiness by only a small degree.

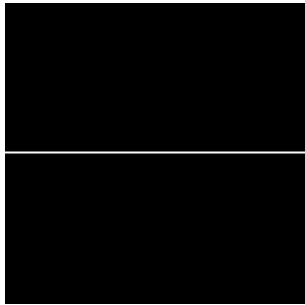


Figure 3a. Ideal delta-width filament



Figure 3b. Filament convolved with PRF r

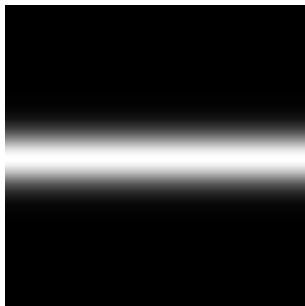


Figure 3c. Filament convolved with PRF p



Figure 3d. MCS Deconvolution of Filament

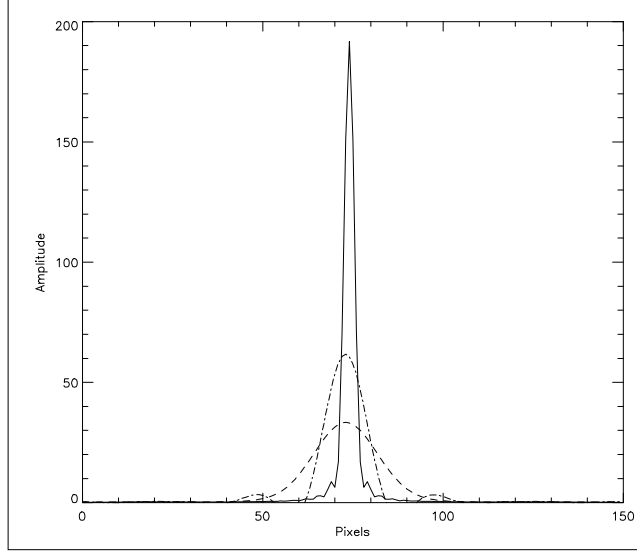


Figure 4. Cross section – MCS Reconstruction of filament

This is demonstrated in Figures 3 and 4, which show the reconstruction of a linear feature using the MCS regularization. Figures 3a-d show the (a) ideal data of a single delta-function width filament, (b) the filament convolved with the Airy function PRF \mathbf{r} of a large aperture optical system with diffraction limited pixel size, (c) the “data” image with a Gaussian PRF \mathbf{p} representing in a small aperture low resolution optical system not sampled for diffraction limited performance, and (d) the MCS reconstruction of the filament. In Figure 4 a cross section across the feature is plotted, with the solid line a cross section from image 3b, the dashed line from 3c, and the dash-dot line showing the MCS deconvolution in Figure 3d. The feature width of the deconvolved filament is slightly narrower than the original image, FWHM of ~ 12 pixels versus the original 19 of the Gaussian blur, and with slightly enhanced amplitude. The reconstruction does not accurately represent the true feature width or amplitude of the system we are trying to model or the single pixel width of the original filament.

4. INVESTIGATING REVISED REGULARIZATIONS FOR MCS

It would be useful to derive a new regularization term for the MCS super-resolution algorithm that enhances the ability of the method to (1) accurately reconstruct the position, thickness and amplitude of filamentary features and (2) resolve linear fine structure to a similar degree as MCS resolves point sources. The theoretical work of Donoho [2] suggests that the super-resolution in one dimension should, under some conditions, be possible. In particular, Donoho proved that a super-resolved solution, \mathbf{x} with dimension n , is admitted for cases where \mathbf{x} has $\leq (m-1)/2$ non-zero elements. In this case the original low-resolution data, \mathbf{y} has m elements. This condition is easily satisfied in one-dimensional spectra composed of discrete lines, or in 2-D images composed of point sources. Donoho notes that the existence of a solution is strongly dependent on the spacing of the non-zero elements, but since the 1-D filament in a 2-D image case can be re-cast as a 1-D problem, the lack of spacing along the filament axis is not a problem, though it does rule out the super-resolution of structure along the filament axis. It should allow the resolution of linear filaments in a 2-D image. However, since the number of non-zero elements will be much larger than the point source only case, the condition will be harder to meet

In the point source case, we begin with an $m=M \times M$ element low resolution image \mathbf{y} . In this case, in the ideal image is \mathbf{x} , where the point sources are delta functions, and the number of non-zero elements in \mathbf{x} is the number of point sources. We will take our representation of \mathbf{x} to have $n=N \times N$ elements. Since Donoho proves there must be a solution if fewer than $(m/n)/2$ elements of \mathbf{x} are non-zero, we see as the number of point sources increases, if we are to maintain the super-resolution condition, we would need to increase the number of samples in n in \mathbf{x} , which is equivalent to saying that the Rayleigh distance, shown by Donoho to be equivalent to n/m , that can be resolved must increase. This would imply that the ability to super-resolve sources in a crowded field depends on the spacing between sources and we can resolve closer objects if we start with a better optical system. This is not surprising and Donoho also makes the point that the practical ability to perform super-resolution depends strongly on object spacing within the Rayleigh interval.

For linear filaments, the number of non-zero elements will be much larger than in the point source only case, since the non-zero elements will be given by the number of pixels long each filament is (assuming the filaments have a delta-function defined width (i.e. 1 pixel) in the ideal image \mathbf{x}). Therefore, it is akin to the crowded field point source case, and we find that the spacing between filaments that we will be able to resolve will be (1) much less than that of an equivalent number of point sources and (2) dependent on the length of the filament. Still we should be able to super-resolve filaments to a Rayleigh distance of n/m as long as the number of filamentary pixels is less than $(m-1)/2$.

Since resolving filamentary structure within low resolution images should be theoretically possible, we need to find a regularization scheme that finds and preserves peaks in the data, rather than smoothing them. A regularization idea that suggests itself is to use edge detection techniques in the regularization term. Filament locations should reveal themselves as local maxima in the original image, and edge detection techniques would enhance these features. Giovanelli and Coulais [5], for example, examine MCS style algorithms and use two regularization terms, one a nearest neighbor pixel difference and the other a Tikhonov regularization. The nearest neighbor difference essentially acts in this fashion as a crude edge detection filter. As part of this work I have examined the Laplacian of Gaussian (LoG) filter as a potential regularization term that would enhance structure in the image. However, since this and other edge detection filters key on changes in the sign of the derivative, therefore it not only resulted in enhanced peaks, but for the thickened features in the low resolution image, filamentary structure yielded 3 edges – two and the filament edge and one at the peak, resulting in spurious structure.

Since edge detection was not compatible for regularization of low resolution images, I tried an exponential form

$$\lambda H = \lambda \sum (\mathbf{h} - \exp[s \otimes h]) \cdot \sum h' / \sum \exp[s \otimes h]$$

that is normalized by the total background flux in order to preserve the image photometry. This regularization will enhance feature peaks within the low resolution data, but drive them to narrower widths than in the original image data.

5. EXPONENTIAL REGULARIZATION – SINGLE FILAMENT

The first question to be answered is does the exponential regularization give better performance for the background that can be reconstructed for a low resolution system than the MCS resolution as in Figures 3 and 4. Using the exponential regularization, we get the results shown in the Figure below. For a single filament, the exponential regularization vastly outperforms the standard regularization term, recovering a filament width only slightly wider than the PSF \mathbf{r} of the diffraction limited system being modeled.



Figure 5. Super-resolution of Filament with Exponential Regularization

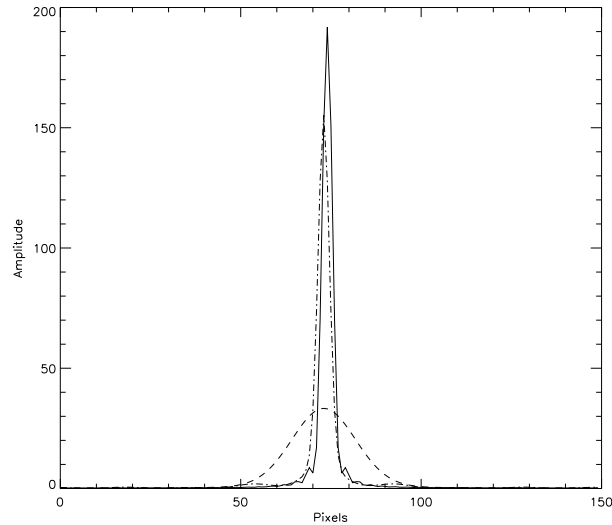


Figure 6. Cross Section of Filament from Figure 5

6. EXPONENTIAL REGULARIZATION – DOUBLE FILAMENT

The final question to be answered is will the exponential regularization allow the MCS reconstruction to resolve two filaments that merge at the original system resolution, and at what point does the ability to resolve filaments break down. For the system with a Gaussian blur, we follow the general rule that if the centroids of the Gaussians are separated by the FWHM, we can resolve two objects. The $\text{FWHM} = 2.35\sigma$ for a Gaussian. In the examples below, sigma is 8 pixels, which yields a FWHM of 18.8 pixels.

In order to test the ability of the exponential regularization to perform super-resolution, we tested linear filaments separated by 20, 15, and 10 pixels. The figures below plot a column of the image data perpendicular to the filaments in order to show the ability of the method to resolve the structures. The solid line represents filaments as they would appear to the “ideal” system with PSF \mathbf{r} that we are attempting to model with the MCS super-resolution. The dashed line is the blurred image with the Gaussian PSF, which supplies the image data, \mathbf{d} , for the MCS input. The dash-dot line is the deconvolution using the MCS method with exponential regularization.

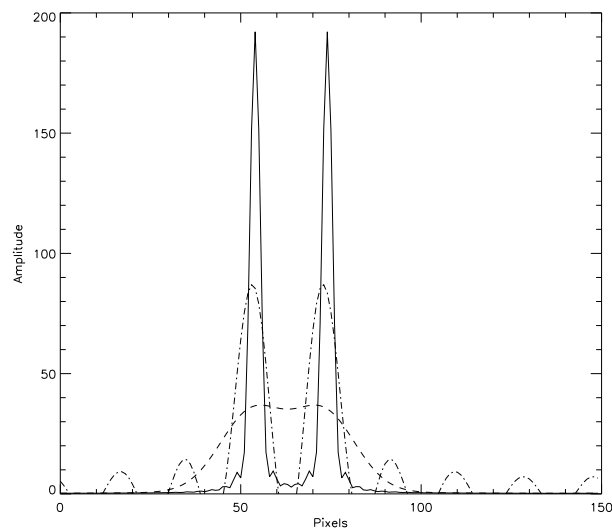


Figure 7. Two Filaments - 20 pixel spacing

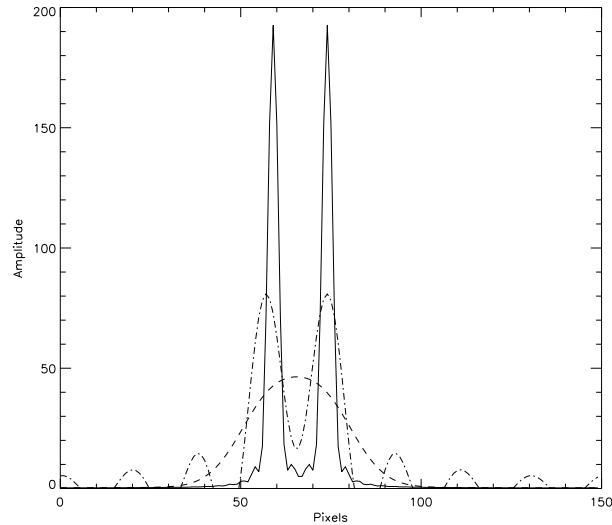


Figure 8. Two Filaments - 15 pixel spacing

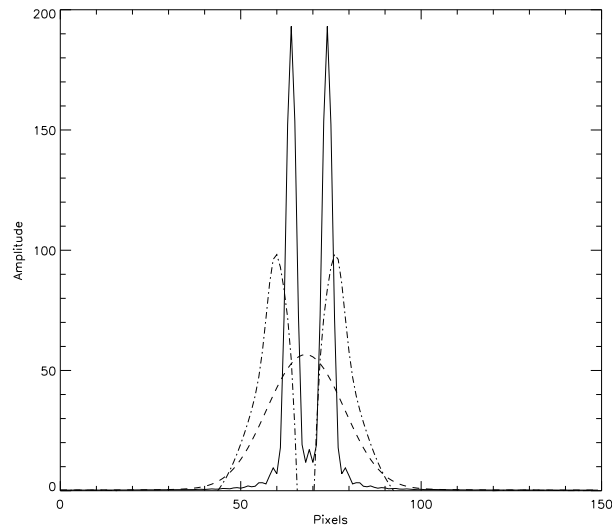


Figure 9. Two Filaments - 10 pixel spacing

The exponential regularization achieves a degree of deconvolution even when the distance between filaments is less than the FWHM of the PSF, achieving actual super-resolution of the images, and arriving at positions of the filament centroids within a pixel or two of the true value. In some cases the method has introduced ringing parallel to the filament at lower background levels, although this also happens at times for the MCS solution and is not directly related to the regularization method. Using the original MCS regularization we do not achieve separation of the filaments when they are closer than the FWHM of the blur. The reconstruction is not as good as the performance seen for the single filament case, but this is to be expected given the theoretical considerations of super-resolution.

7. CONCLUSIONS

Under certain conditions, the super-resolution of linear filaments is possible within the constraints of Donoho's proof of super-resolution. While this does not generally allow super-resolution (as opposed to contrast enhancement) in the general area of 2-D images, it may have application in astronomy where filamentary structures against a black background are common features.

I have also demonstrated that revising the regularization term in the MCS 2-channel image deconvolution method to an exponential function enhances peakiness in filaments, and allows some degree of super-resolution for filaments near the resolution limit of the original imaging system. Performance like that for point sources was not achieved, but this regularization method may be most useful where a-prior knowledge of the position of filaments is known.

REFERENCES

1. Puschmann, K.G. and Kneer, F., On super-resolution in astronomical imaging, *Astronomy & Astrophysics*, Vol 436, 373-378, 2005.
2. Donoho at el., *Journal of the Royal Statistical Society*, Vol. 54, 41, 1992.
3. Magain, P., Courbin, F., Sohy, S., Deconvolution with Correct Sampling, *The Astrophysical Journal*, Vol. 494, 472-477, 1998.
4. Egan et al., Testing the MCS Deconvolution Algorithm on Infrared Data ,*AMOS Conference Proceedings*, 2007.
5. Giovannelli, J.-F., and Coulais, A., Positive deconvolution for superimposed extended source and point sources, *Astronomy & Astrophysics*, Vol 439, 401, 2005.